JOURNAL OF MATERIALS SCIENCE **36** (2001) 2621 – 2632

Atomic force microscopy studies of short melamine fiber reinforced EPDM rubber

R. S. RAJEEV, S. K. DE, A. K. BHOWMICK*
Rubber Technology Center, Indian Institute of Technology, Kharagpur 721 302, India

G. J. P. KAO, S. BANDYOPADHYAY
School of Materials Science and Engineering, University of New South Wales, Sydney 2052, Australia

Atomic Force Microscopy (AFM) was used to investigate the morphology and interfacial properties of unaged and aged Ethylene Propylene Diene (EPDM) rubber-melamine fiber composites. Interfacial adhesion between the fiber and the matrix was weak in the absence of a dry bonding system consisting of hexamethylene tetramine, resorcinol and hydrated silica (HRH). AFM images revealed the formation of an interface between the fiber and the matrix with the addition of the bonding agents. Ageing of the composites improved the adhesion between the fiber and the matrix, which was evident from the topographic images of the aged composites. It was found that two-dimensional and three-dimensional topographic images from AFM could be used to determine fiber geometry, fiber diameter and fiber-matrix adhesion in short fiber-rubber composites.

1. Introduction

Short fiber reinforced elastomers combine the rigidity of fiber with the elasticity of rubber [1]. One of the main advantages of reinforcing elastomers with short fibers is that the fiber can be incorporated as one of the compounding ingredients during the mixing process. Properties of short fiber filled rubber composites primarily depend on the existence of a good fiber-matrix adhesion [2]. An optimum aspect ratio and uniform orientation of fibers are also significant for the effective reinforcement of elastomers using short fibers [3]. One of the most widely used techniques for accomplishing good fiber-matrix adhesion is the use of a three component dry bonding system consisting of hexamethylene tetramine, resorcinol and hydrated silica, popularly known as HRH dry bonding system. Several authors have studied the effect of dry bonding system in a variety of short fiber-rubber composites. Derringer [4] used HRH dry bonding system with various fibers in nitrile and natural rubbers. Murty and De [5] found that there exists an optimum ratio of the constituents of the dry bonding system for the effective reinforcement of natural rubber with short jute fibers. Setua and De [6] observed that in order to acquire optimum properties, all the three components of the dry bonding system must be present together. Ibarra and Chamorro [2] used natural magnesium silicate in place of silica in short carbon and polyester fiber reinforced EPDM rubber. In short fiber-rubber composites, though fiber orientation and fiber aspect ratio can be measured using microscopic techniques like scanning electron microscopy and optical microscopy, fiber-matrix adhesion can only be estimated using indirect methods like swelling, measurement of green strength and visco-elastic properties [2].

The development of Atomic Force Microscopy (AFM) [7] has revolutionized the surface science by making it possible to image surfaces on extremely small scales (<1 nm), as well as to measure the forces that dominate adhesion phenomena. AFM is a powerful tool for obtaining high resolution surface topography [8–12]. AFM is widely used in the field of polymer, because properties of polymeric materials are mainly governed by their composition, morphology and interfacial structure. In a recent review, Tsukruk [13] illustrates the basic principles and results of AFM studies of polymer surfaces. The use of AFM in investigating the morphology of block co-polymers is elucidated by Ghosh *et al*. [14]. They have studied the surface morphology of molded thin films of segmented polyamides using AFM and distinguished the hard polyamide blocks and the soft polyether segments in the copolymer. Joni and Antti [15] have investigated the surface morphology of melt spun polypropylene filaments using AFM and found that during stretching, there is a gradual transformation of surface morphology from a spherulitic morphology to a fibrillar morphology. Rebouillat and coworkers [16] have employed AFM to study the surface structure of Kevlar fibers. Several authors have also reported the use of AFM in the study of microstructure and microdispersion of carbon black [17–21]. Donnet *et al*. [22] have practiced AFM

* Author to whom all correspondence should be addressed.

for the three-dimensional imaging of isolated carbon black aggregates. AFM has also been employed in the studies of elastomers and elastomer blends. Haeringen *et al*. [23] have used AFM to investigate the morphology, filler distribution and adhesion of elastomers using chemically modified tips. They found that tapping mode phase imaging was useful for imaging of the filler aggregates and for the visualization of single primary filler particles. Ganter and coworkers [24] have utilized AFM in the studies of poly(propylene)/poly(1-olefine) blends and BR/SBR blends. They found that AFM could provide information about the morphology of the immiscible rubber components. Mass *et al*. [25] have examined crosslinked BR/IR, SBR/IR and SBR/BR using AFM and imaged features of phase morphology using lateral force mode AFM. In the present study, AFM is used to analyze the fiber dimensions, morphology and fiber-matrix adhesion in short melamine fiber reinforced EPDM rubber. Melamine fiber is a new class of high strength synthetic fiber having good heat and flame resistance. There is also no report on the melamine fiber reinforced rubber composites.

2. Experimental

2.1. Preparation of the composites

Formulations used in the present study are given in Table I. The masterbatches were prepared by mixing the ingredients in a Brabender Plasticorder, model PLE-330 at 80°C and at a rotor speed of 30 rpm. The fiber, in the pulp form, was separated manually and added in small increments in order to obtain uniform dispersion. After incorporation of all the ingredients, rotor speed was increased to 60 rpm and mixing continued for additional 3 minutes. Then the hot mix was taken out, sheeted out in a laboratory two-roll mill at a friction ratio of 1 : 1.2. The mixes were rolled along the mill direction before each pass and then re-sent through the mill. For physical testing, sheets having dimension 145 mm × 120 mm × 2 mm were cured in a hydraulic press at 150°C and 5 MPa pressure for their optimum cure times, determined using a Monsanto Oscillating Disc Rheometer (ODR 100S).

TABLE I Formulations of the mixes A to D

Mix	A	B	C	D
EPDM	100	100	100	100
ZnO	5	5	5	5
Stearic acid	1	1	1	1
Antioxidant[1]	1	1	1	1
Resorcinol	5	0	5	10
Hexamine	3	0	3	6
Silica	15	0	15	15
Fiber	0	10	10	10
MBT[2]	1.5	1.5	1.5	1.5
TMTD[3]	1	1	1	1
Sulfur	1.5	1.5	1.5	1.5

1 polymerized 2,2,4-trimethyl 1,2-dihydro quinoline.
2 2-mercaptobenzothiazole.
3 tetramethyl thiuram disulfide.

2.2. Measurement of physical properties

The stress-strain properties were measured according to ASTM D 412-98a specification using dumb-bell test pieces in a Zwick Universal Testing Machine (UTM, model 1445) at a crosshead speed of 500 mm/min. In order to study the fiber orientation, samples were cut with fibers oriented along the milling direction (longitudinal) and across the milling direction (transverse) and properties of samples with both longitudinally and transversely oriented fibers were determined. The hardness was determined as per ASTM D 2240 (1997) and expressed in Shore A units.

2.3. Ageing studies

Ageing studies were performed by determining the mechanical properties after ageing the test specimens at 150°C for 48 hours in a circulating ageing oven. Prior to testing the aged samples were conditioned at room temperature for 24 hours.

2.4. Scanning electron microscopy

The tensile fracture surfaces were sputter coated with gold and then examined under JEOL Scanning Electron Microscope, model JSM 5800.

2.5. Atomic force microscopy (AFM) studies

For AFM imaging, specimens were prepared by cryomicrotoming using liquid nitrogen. Average sample thickness was 20 μm. The AFM measurements were carried out in air at ambient conditions (25°C) with a Nanoscope III Atomic Force Microscope, made by Digital Instruments Inc., USA. The experiments were carried out in the tapping mode with constant amplitude, using microfabricated cantilevers. The scanning was done using etched silicon tip, square pyramid in shape, with a base dimension of approximately 4 μm × 4 μm. The characteristics of the probes are: Spring constant (K) 0.58 N/m; Nominal tip radius of curvature, 20 nm; Cantilever length, 100 μm; Cantilever configuration, V shaped; Reflective coating, gold; Sidewall angles, 30° on all four sides. Images were analyzed using a Nanoscope image processing software. All images contained 256 data points.

3. Results and discussion

3.1. Mechanical properties of the composites

Table II gives the mechanical properties of the mixes A, B C and D. The properties of the mixes obtained after ageing the samples at 150°C for 48 hours are given in brackets. The role of the dry bonding system in improving the adhesion between the fiber and the matrix is apparent from the comparison of the mechanical properties of the composite without bonding agent (mix B) and that with bonding agent (mix C). Without bonding agent, the composite is very weak, having tensile strength of only 1.7 MPa. Addition of resorcinol, hexamine and silica in the ratio 5 : 3 : 15

TABLE II Mechanical properties of mixes A to D[a]

Mix		A	B	C	D
Resorcinol/hexamine loading (phr)		5/3	0	5/3	10/6
Silica loading (phr)		15	0	15	15
Fiber loading (phr)		0	10	10	10
Tensile strength (MPa)	L[b]	4.2 (3.4)	1.7 (2.0)	4.5 (4.9)	5.1 (6.3)
	T[b]	4.2 (3.4)	1.3 (1.4)	4.1 (4.2)	4.7 (5.7)
Elongation at break (%)	L	250 (149)	146 (83)	191 (111)	208 (121)
	T	250 (149)	149 (76)	211 (115)	227 (121)
Modulus at 100% elongation (MPa)	L	1.6 (2.2)	1.3 (−)	3.2 (4.6)	3.2 (5.4)
	T	1.6 (2.2)	1.2 (−)	2.5 (3.5)	2.6 (4.7)
Hardness (shore A)		53 (61)	53 (61)	60 (66)	60 (66)

[a]- Values in the brackets indicate properties obtained after aging the composites at 150°C for 48 hours.
[b]- L stands for longitudinally oriented fibers; T stands for transversely oriented fiber.

significantly improves the mechanical properties of the composites when tensile strength and modulus are increased about 3 times as compared to the composite without bonding agent. It is interesting to note that melamine fiber, which is in the pulp form, brings about anisotropy in mechanical properties after processing. Tensile strength is marginally greater in the longitudinal direction than in the transverse direction and as anticipated elongation at break displays the opposite trend. Modulus also shows the anisotropic behavior. Anisotropy in mechanical properties of short fiber reinforced composites is known to be displayed more prominently by modulus at low elongation than tensile strength. Also the preferential orientation of fibers in the milling direction is more prominent if the fibers are well bound to the matrix by means of bonding agents. Therefore, the composites with dry bonding system (mixes C and D) produce a greater anisotropy in properties compared to the composite having no bonding agent (mix B).

The role of fiber in improving the modulus and strength of the composite is further evident on comparing the tensile strength and modulus of the mix A (without fiber) and mix C (with 10 phr fiber), both containing the same ratio of bonding agents. Though tensile strength is increased only marginally by the incorporation of fiber (possibly due to the low fiber concentration), modulus is increased notably by the addition of fibers. The increase in modulus of the composite is mainly due to the presence of fibers, which are having a modulus always higher than that of the matrix (that is, 7 GPa for fiber and 3 MPa for rubber matrix). The hardness of the composites is also increased due to the presence of fibers.

Table II also shows that as resorcinol/hexamine ratio is increased from 5 : 3 to 10 : 6(that is, mixes C and D) there is a corresponding increase in tensile strength and elongation at break of the composites. It is observed that for EPDM-melamine fiber composites, a higher ratio of bonding agent is needed for optimum mechanical properties compared to other short fiber rubber composites like natural rubber-jute fiber [5], natural rubber-silk fiber [6] and EPDM-aramid fiber [26]. Increase in the ratio of bonding agents induces no change in the hardness of the composites, which indicates that the increase

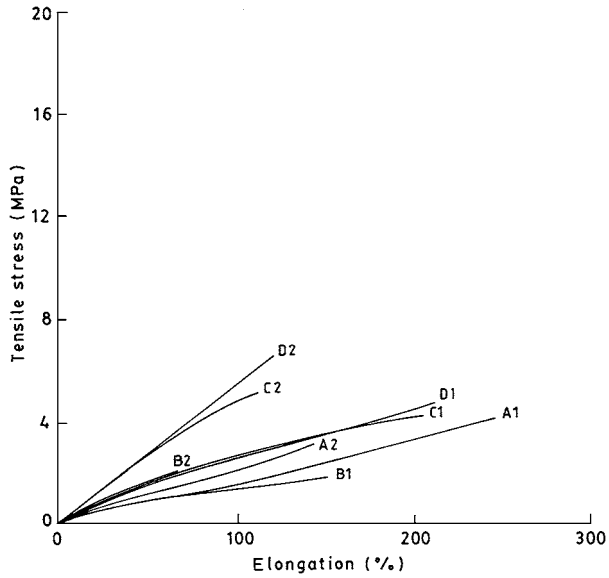

Figure 1 Stress-strain curves of the composites. A1-mix A unaged; A2-mix A aged; B1-mix B unaged; B2-mix B aged; C1-mix C unaged; C2-mix C aged; D1-mix D unaged; D2-mix D aged.

in strength is mainly due to the improved interaction between the fiber and the matrix.

Ageing at 150°C for 48 hours causes a distinct change in the mechanical behavior of the composites. Fiber-rubber composites show an increase in tensile strength and modulus after ageing, particularly in presence of bonding agents. In the absence of fiber, ageing causes a drop in tensile strength, but fibers hinders composite deterioration in presence of bonding agent, thus displaying better retention of strength on ageing. The effect of ageing on the stress-strain curves of the composites is shown in Fig. 1. Ageing produces a near-linear stress-strain curve, especially for composites with bonding agent. Elongation of the aged composites decreases considerably compared to the unaged composites. Even in the absence of bonding agent, there is an increase in strength and modulus due to ageing. But addition of bonding agent further increases the strength. It is also observed that as resorcinol-hexamine ratio is increased from 5 : 3 to 10 : 6, the percent increase in tensile strength and modulus after ageing is also increased,

which again fortifies the observation that as bonding agent ratio is increased, adhesion between the fiber and the matrix is improved.

3.2. Atomic Force Microscopic studies of the composites

Fig. 2 shows the three-dimensional topographic image of mix A (without fiber) in a scan area of $5 \times 5\ \mu m^2$. Mainly two different contrast levels are observed here. The dark background is the rubber matrix. The size of white particles is around 140 ± 40 nm. The formulation contains ZnO as well as silica. Therefore the white particles are presumed to be the aggregates of ZnO and silica particles. Silica particles are not distinguished in this image. Microdispersion of fillers are better understood if AFM is used in conjunction with digital image analysis [18] or phase imaging [23], which allows unambiguous resolution of the different phases. Section analysis of Fig. 2 is given in Fig. 3. Here the particles protruding from the surface are denoted by the inverted triangle. A cross sectional line is drawn across the image and the vertical profile along the line is displayed. Each pair of cursors in the image will give horizontal, vertical and angular measurements of the point of interest. Here the horizontal distance corresponds to the diameter of particles projecting at a height given by the vertical distance from the surface. The average horizontal distance made by the inverted triangles is 280 nm, which is assumed to be the diameter of ZnO and silica particles aggregated together. It can also be noticed from Fig. 3 that maximum vertical distance is only approximately 40 nm and the profile is almost smooth, indicating that in the absence of fiber, the surface is smooth.

Fig. 4 shows the topographic image of the cross section of a typical fiber in the composite. The scan area is $30 \times 30\ \mu m^2$. In AFM, dark areas depict low features and white areas represent high features. Therefore, the white portion in the figure is a projection from the base matrix. The average diameter of the white portion is approximately 16 μm, which corresponds to the diameter of a single melamine fiber [27]. The section analysis of Fig. 4 is given in Fig. 5. The distance along the X-axis between the inverted pair of triangles gives the horizontal distance, which is 16.64 μm corresponding to the diameter of a melamine fiber. Therefore the white surface is nothing but fiber projecting from the rubber matrix. The fiber diameter brought about using section analysis is in agreement with the fiber diameter obtained by Scanning Electron Microscopy (15.20 μm, Fig. 6).

The role of bonding agent in improving fiber-matrix interaction is evident from AFM images. Figs 7 to 9 give the section analyses of composites with resorcinol/hexamine ratio 0 : 0, 5 : 3 and 10 : 6 respectively (mixes B, C and D). It can be observed that in the absence of bonding agent, the width of the interface is only 0.59 μm (Fig. 7). The fiber matrix interface is very smooth, showing little interaction between the fiber and the matrix. When resorcinol and hexamine are added in the ratio 5 : 3, the width of the interface

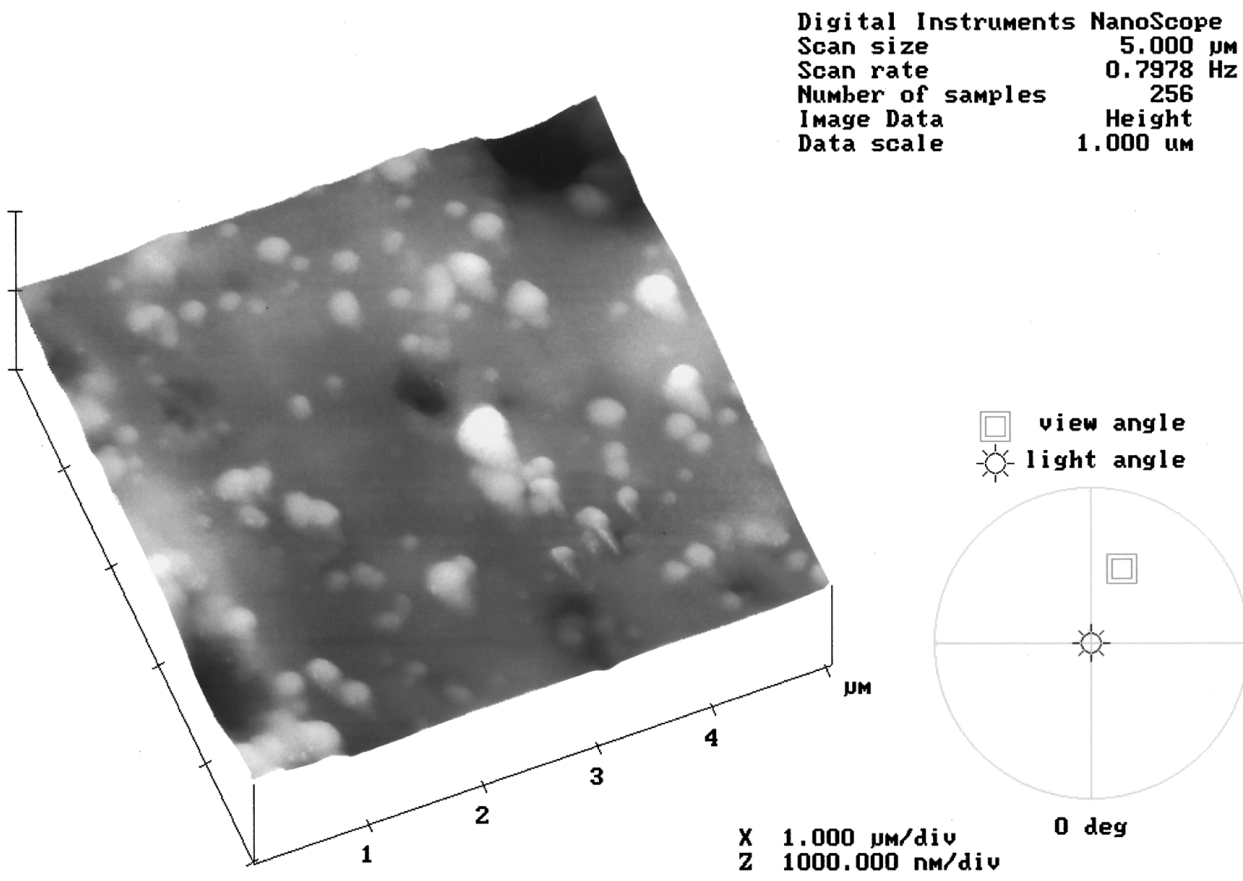

Figure 2 Three-dimensional topographic image of the compound without fiber. White particles are aggregates of ZnO and silica particles.

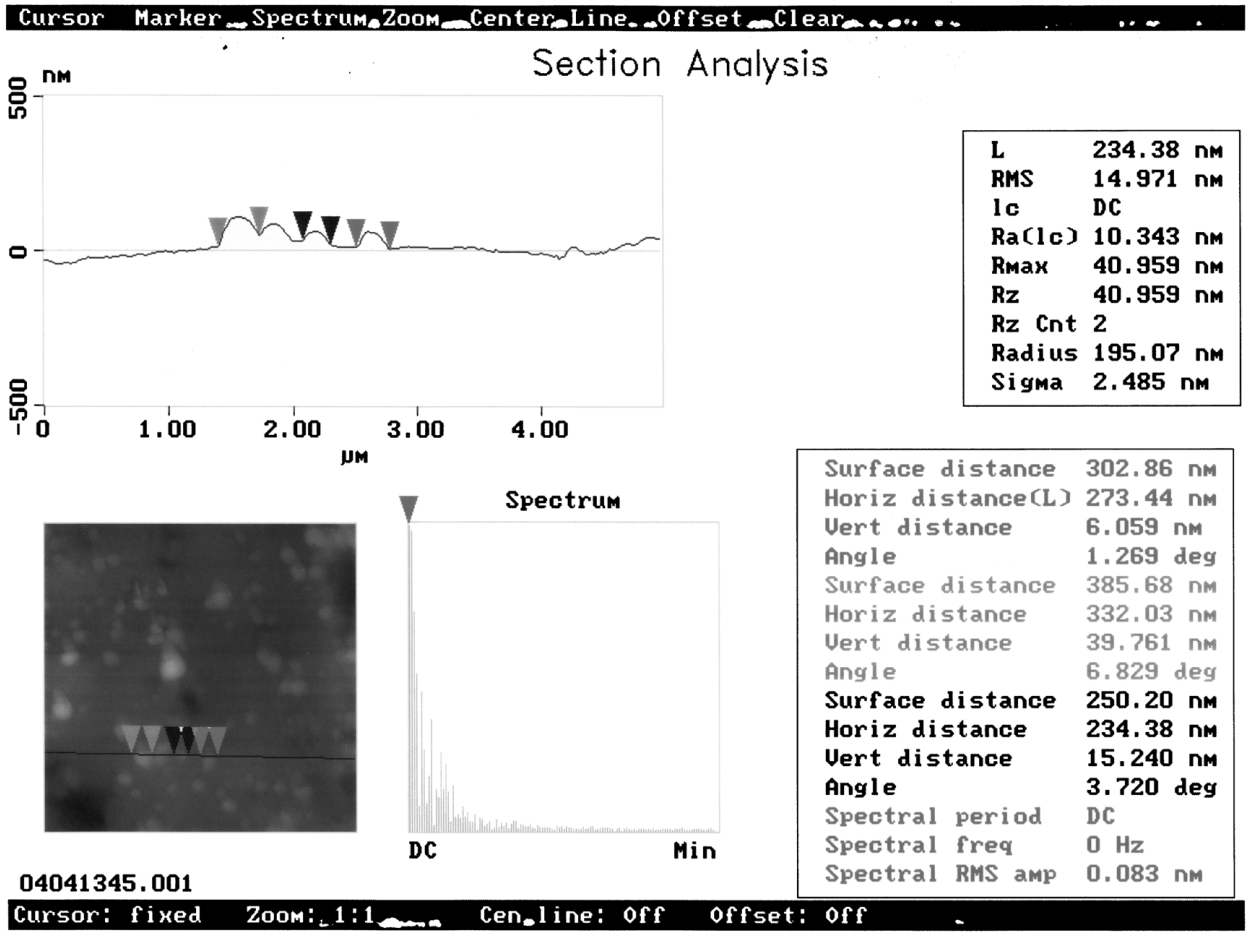

Figure 3 Section analysis of the compound without fiber. Diameter of the particles is measured using inverted triangles.

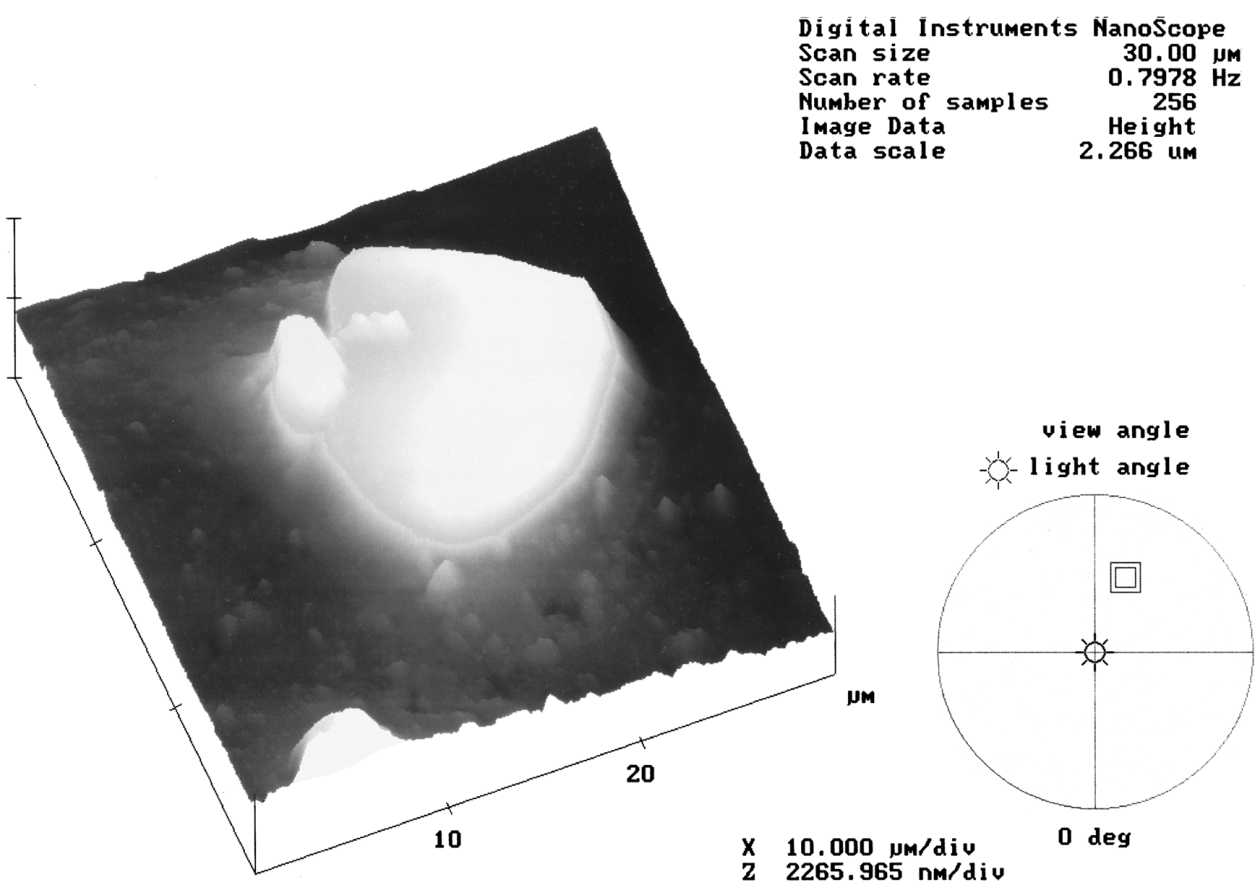

Figure 4 Three-dimensional topographic image of the fiber in the composite.

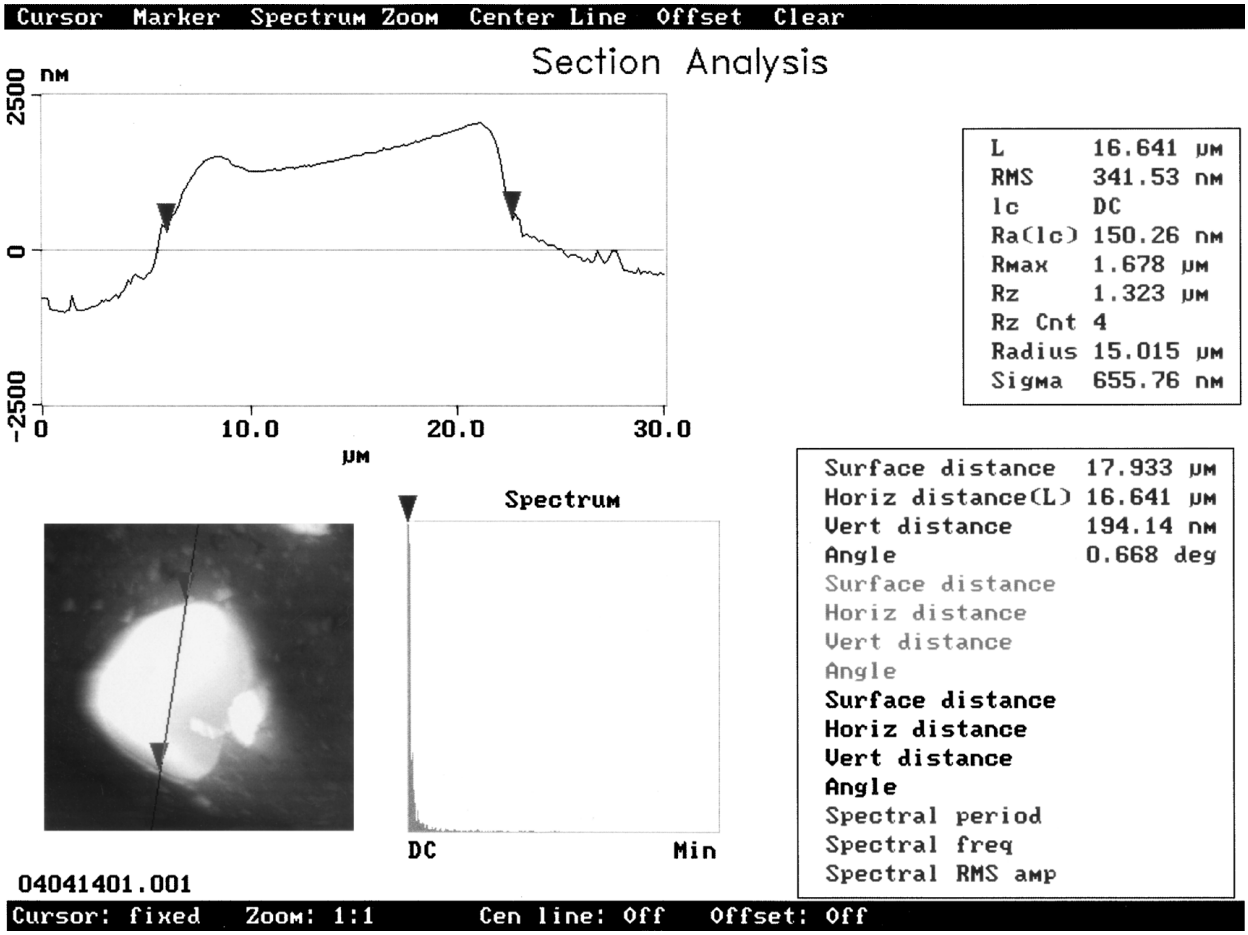

Figure 5 Section analysis of Fig. 3. The horizontal distance between the inverted triangles gives fiber diameter.

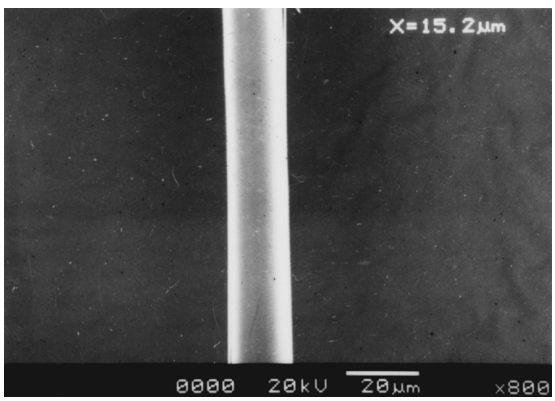

Figure 6 SEM photomicrograph of the fiber in the composite.

is increased to 1.79 μm (Fig. 8). Here the morphology of the interface is changed and also there is an interaction between the fiber and the matrix compared to composite without bonding agent. When the ratio of bonding agent is increased to 10 : 6, the width of the interface is further increased to 5.39 μm (Fig. 9). This shows that as bonding agent ratio is raised, the interface thickness is increased. The mechanical properties described earlier are in line with the increase in interfacial thickness.

Ageing improves tensile strength and modulus of the composites. There is a strong interfacial adhesion between the fiber and the matrix after ageing. Figs 10 and 11 show the SEM photomicrographs of the tensile fracture surfaces of the unaged and aged composites. An absolutely different type of matrix morphology is obtained after ageing. It can be seen that after ageing the matrix is efficiently covering the fiber surface. The unaged fracture surface in Fig. 10 shows that major failure mechanism is fiber pullout from the matrix and subsequent matrix failure. But after ageing, fracture takes place mainly in the matrix plane (Fig. 11). The fiber is fully covered by the matrix so that no fiber pull out is observed here.

AFM images also reveal that although an interface is formed with the addition of bonding agents, the bonding between the fiber and the matrix is not perfect in the case of unaged composites. There is debonding between the fiber and the matrix before ageing. Fig. 12 shows the three-dimensional topographic image of the composite (mix C) before ageing. The debonding between the fiber and the matrix is distinctly visible here. It can be observed that at some portions, the gap between the fiber and the matrix is in the range of 0.74 to 0.93 μm. This distance between the fiber and the matrix is proportional to the extent of debonding. At the interface, the matrix is folded backward and it is not coming well in contact with the

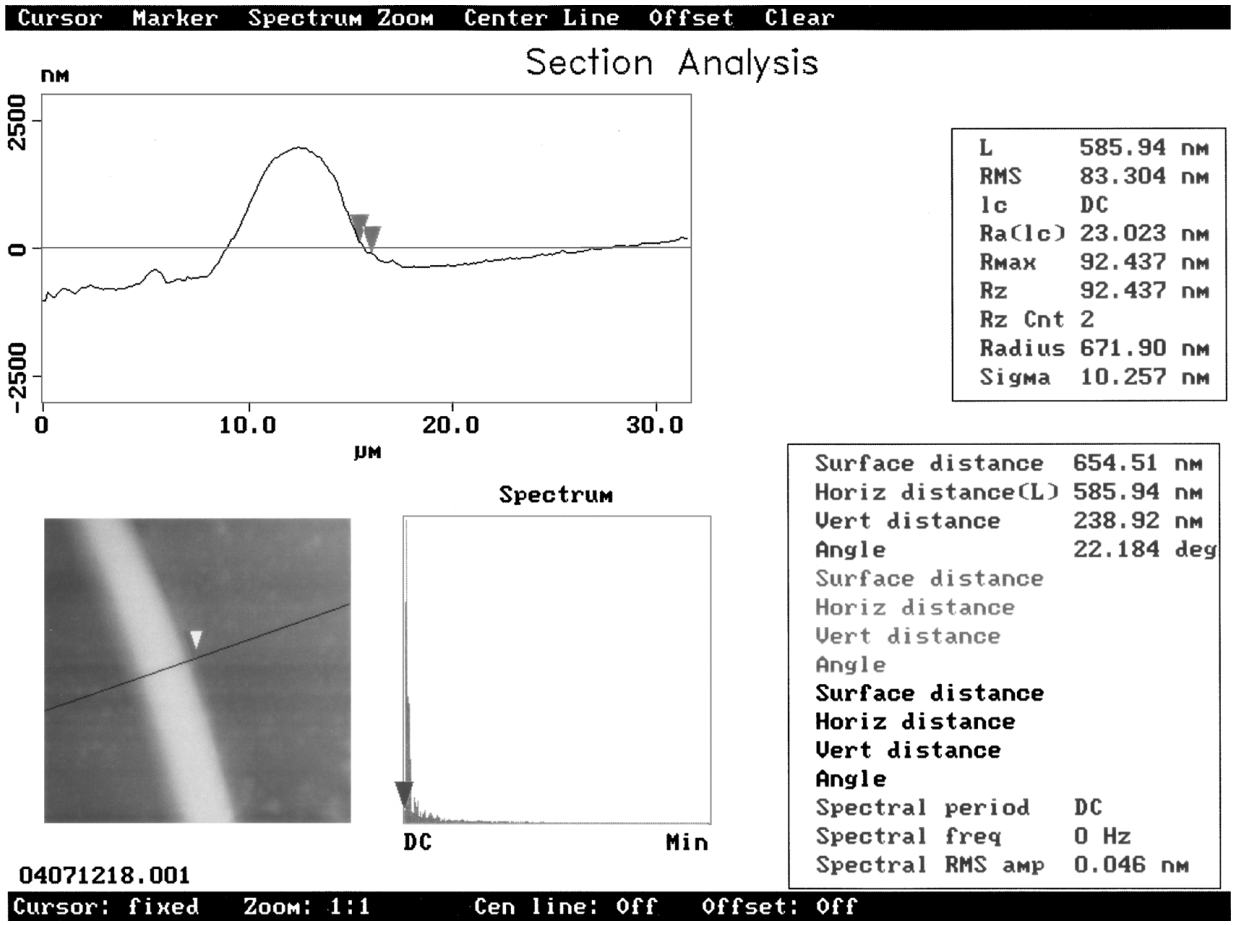

Figure 7 Section analysis of composite without bonding agent. Interface width is low.

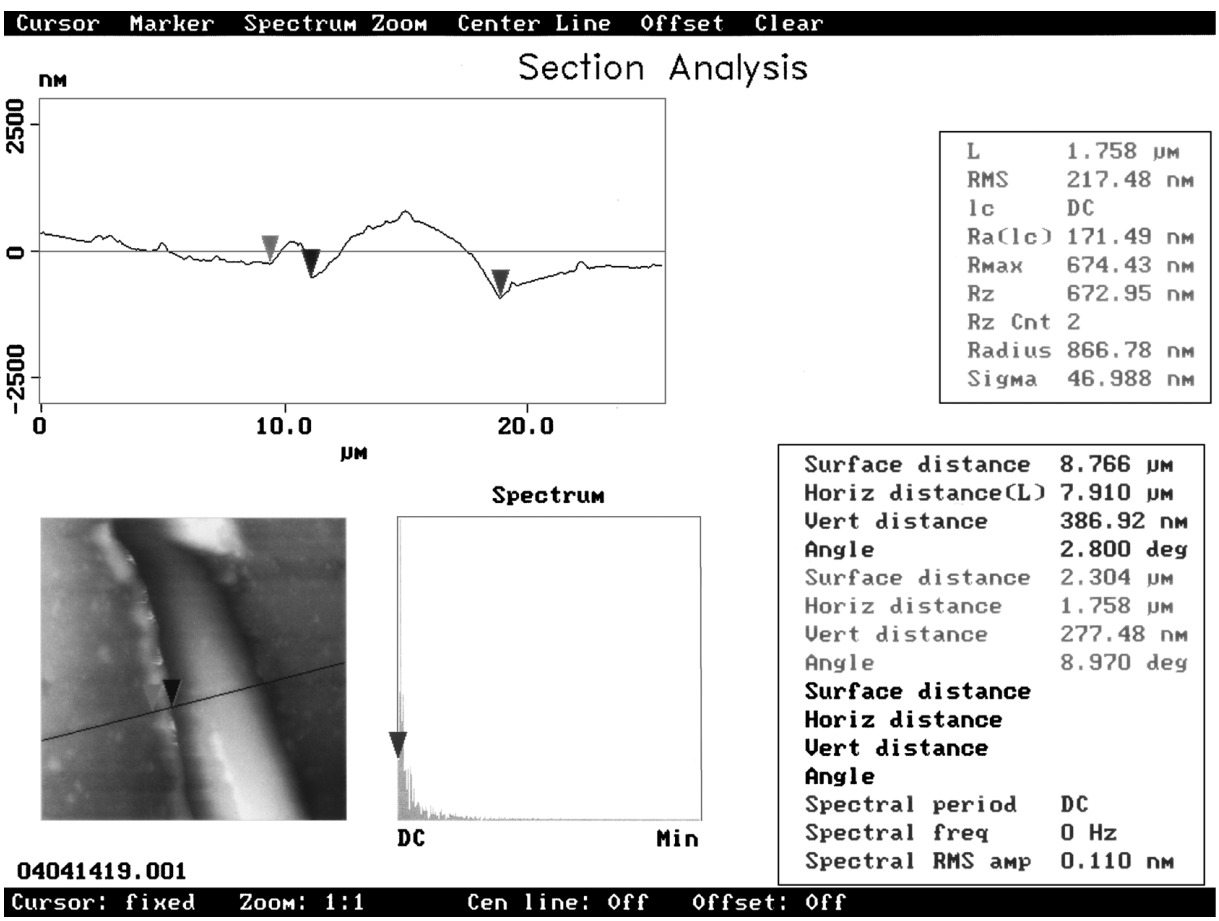

Figure 8 Section analysis of the composite with resorcinol/hexamine ratio of 5 : 3. Width of the interface is higher than that in Fig. 7.

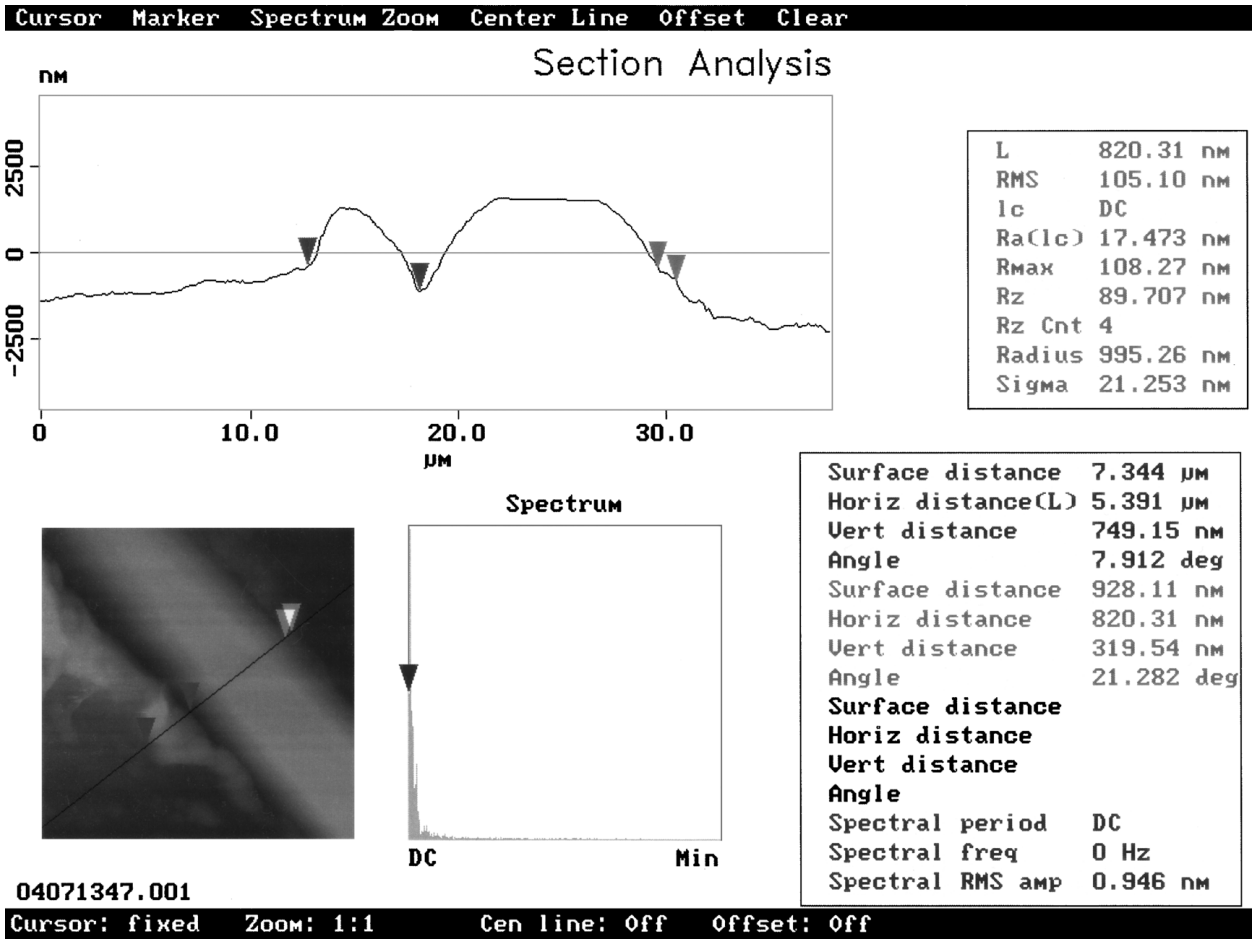

Figure 9 Section analysis of the composite with resorcinol/hexamine ratio of 10 : 6. Higher width of interface shows better fiber-matrix interaction.

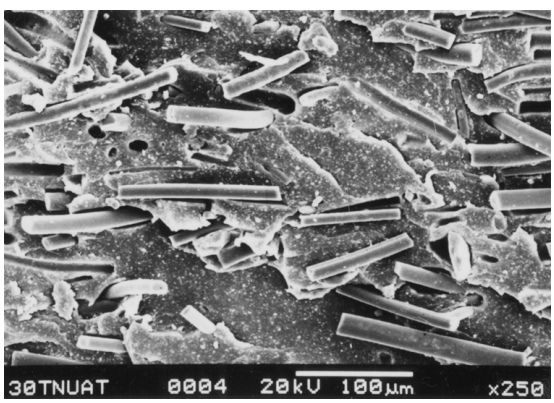

Figure 10 SEM photomicrograph of unaged composite. Debonding and fiber pullout are visible.

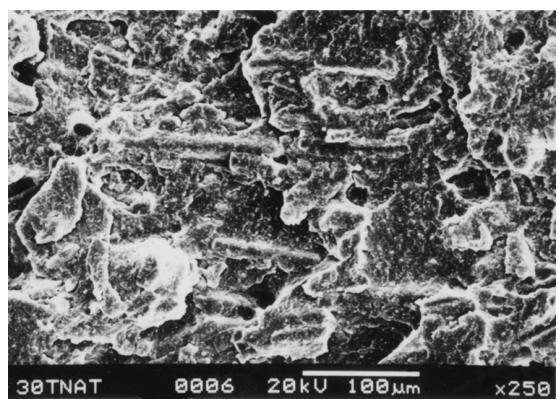

Figure 11 SEM photomicrograph of the composite aged at 150°C for 48 hours. Improved fiber-matrix interaction can be observed.

fiber. The fiber surface is also very smooth, thereby reducing the chances of mechanical interlocking. After ageing, the fiber surface is effectively covered by the matrix, as shown in Fig. 13. This covering of the matrix over the fiber after ageing is evident on comparing the section analyses of the composites before and after ageing (Figs 14 and 15 respectively). Before ageing the fiber surface is smooth but after ageing, due to the greater coverage of the matrix over the fiber, a uniform trace is not obtained over the fiber surface.

The roughness of the surface is also changed after ageing. Figs 16 and 17 respectively give the roughness of the surface before and after ageing. Before ageing, the mean roughness is approximately 62 nm whereas the roughness is reduced to approximately 32 nm after ageing. The reduction in roughness after ageing is due to the uniform coverage of the fiber with the matrix.

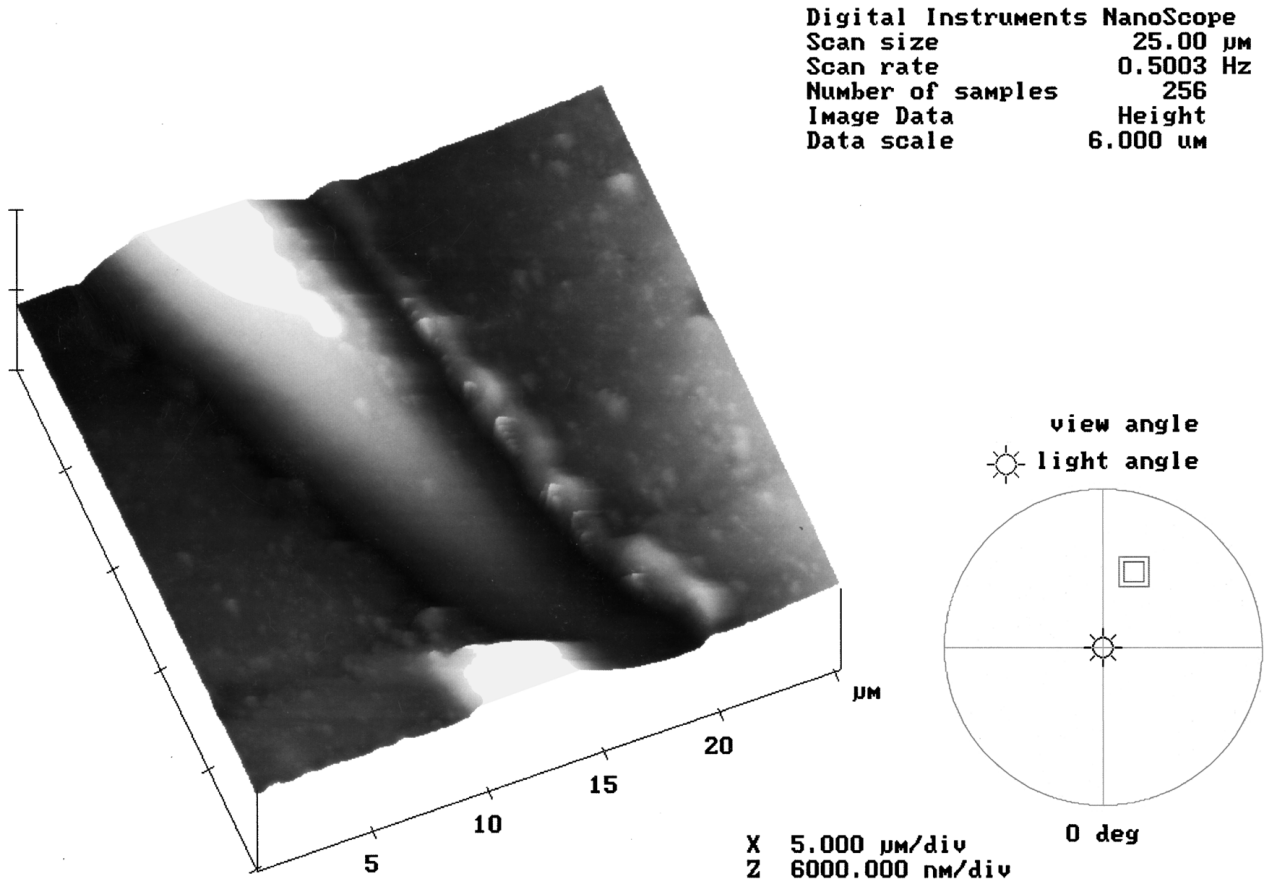

Figure 12 Three-dimensional topographic image of the unaged composite. Debonding between the fiber and the matrix is clearly visible.

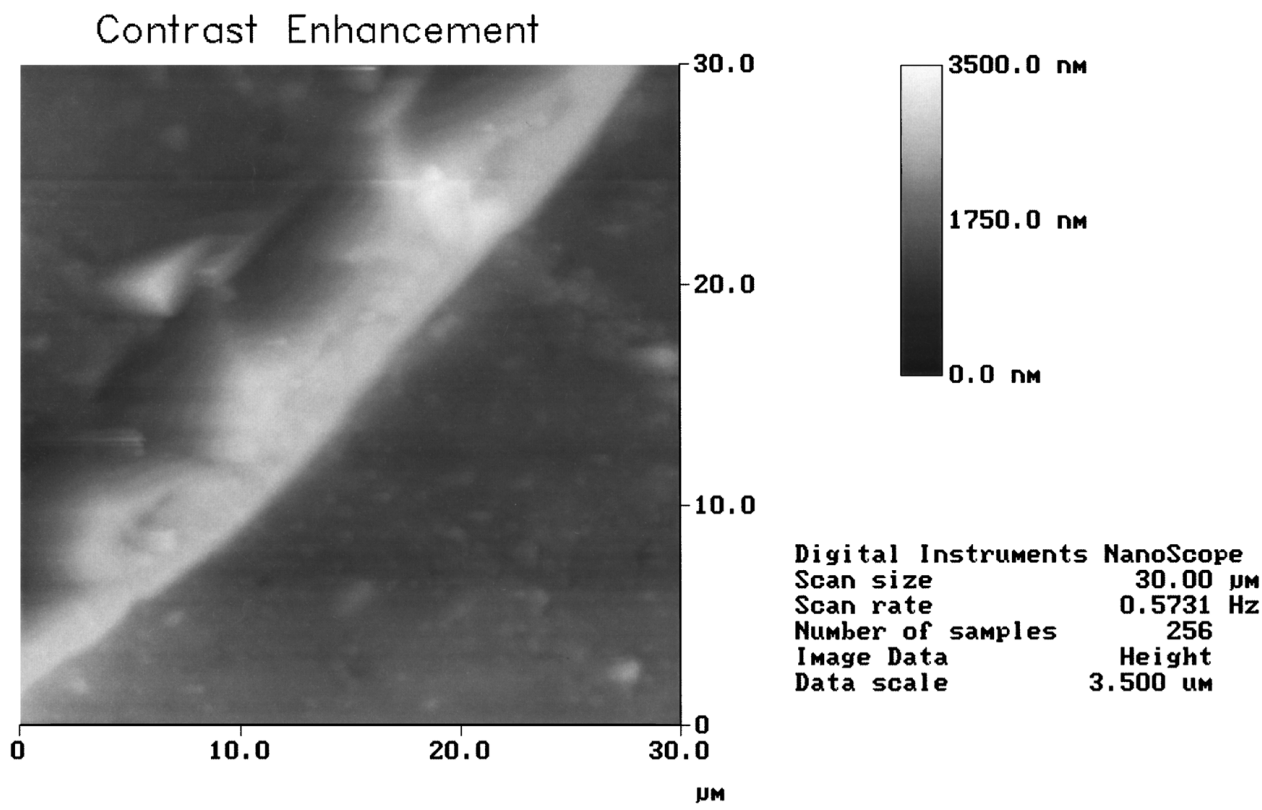

Figure 13 Three-dimensional topographic image of the composite aged at 150°C for 48 hours. Fiber surface is covered by the matrix showing improved fiber-matrix adhesion.

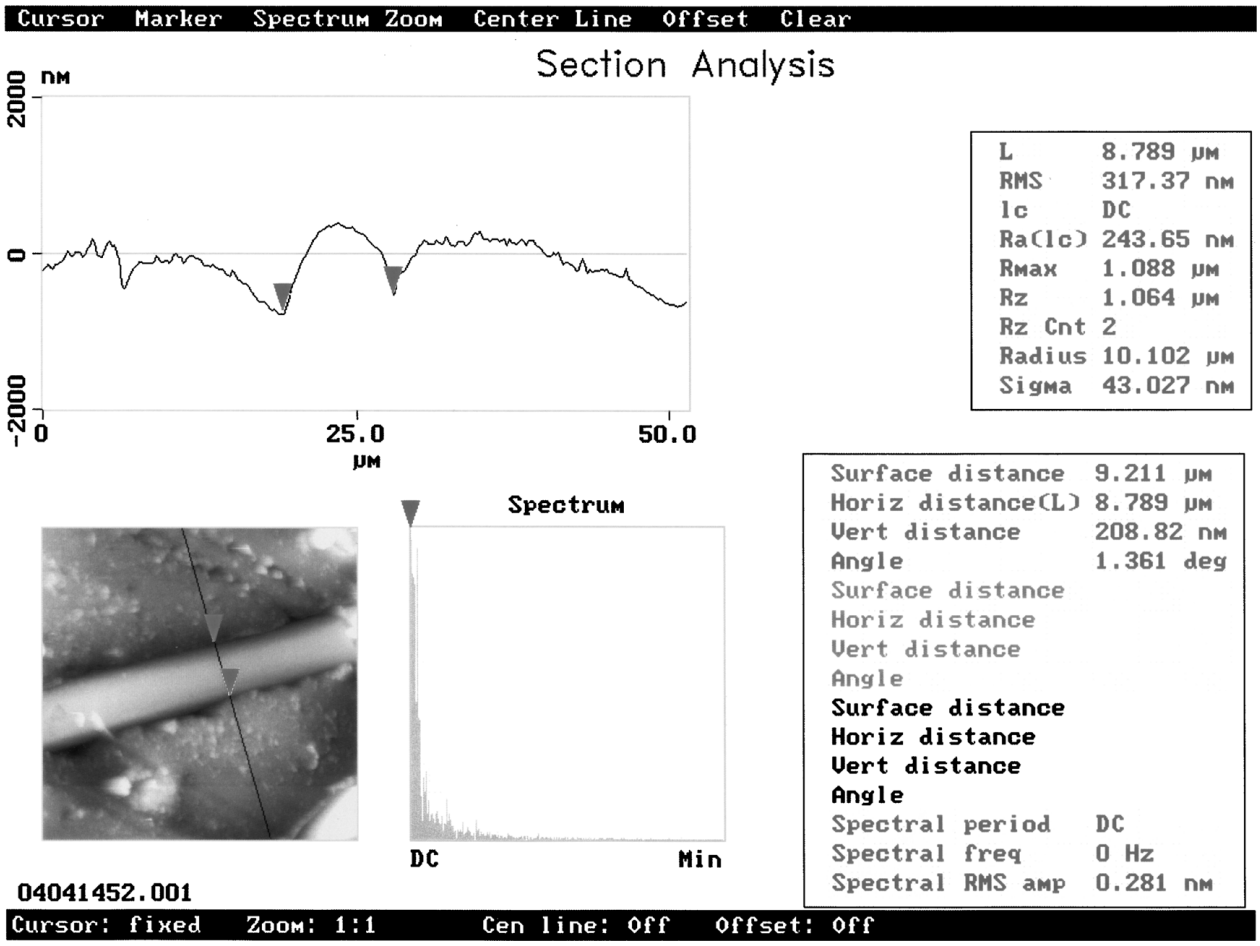

Figure 14 Section analysis of the unaged composite. Trace lines show a smooth fiber surface.

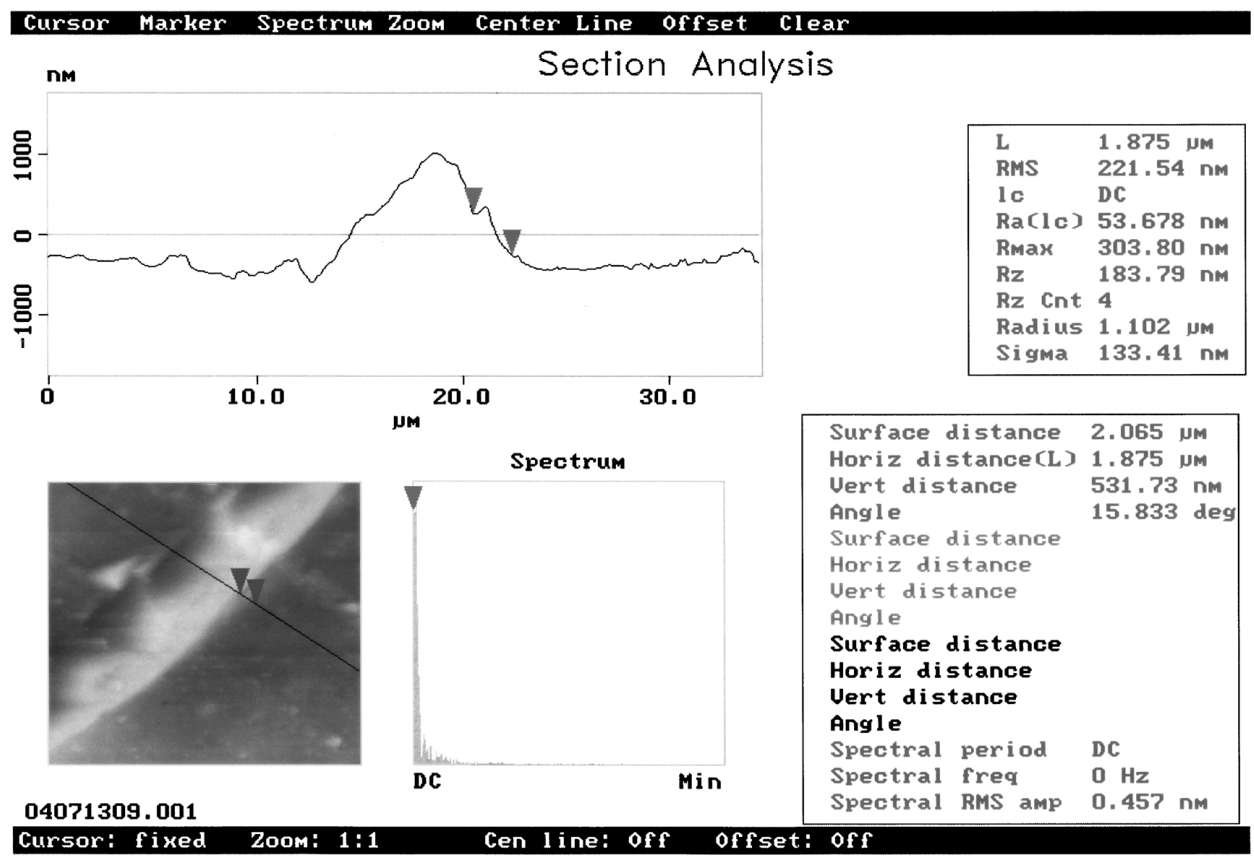

Figure 15 Section analysis of the aged composite. Fiber surface became rough after ageing due to matrix coverage.

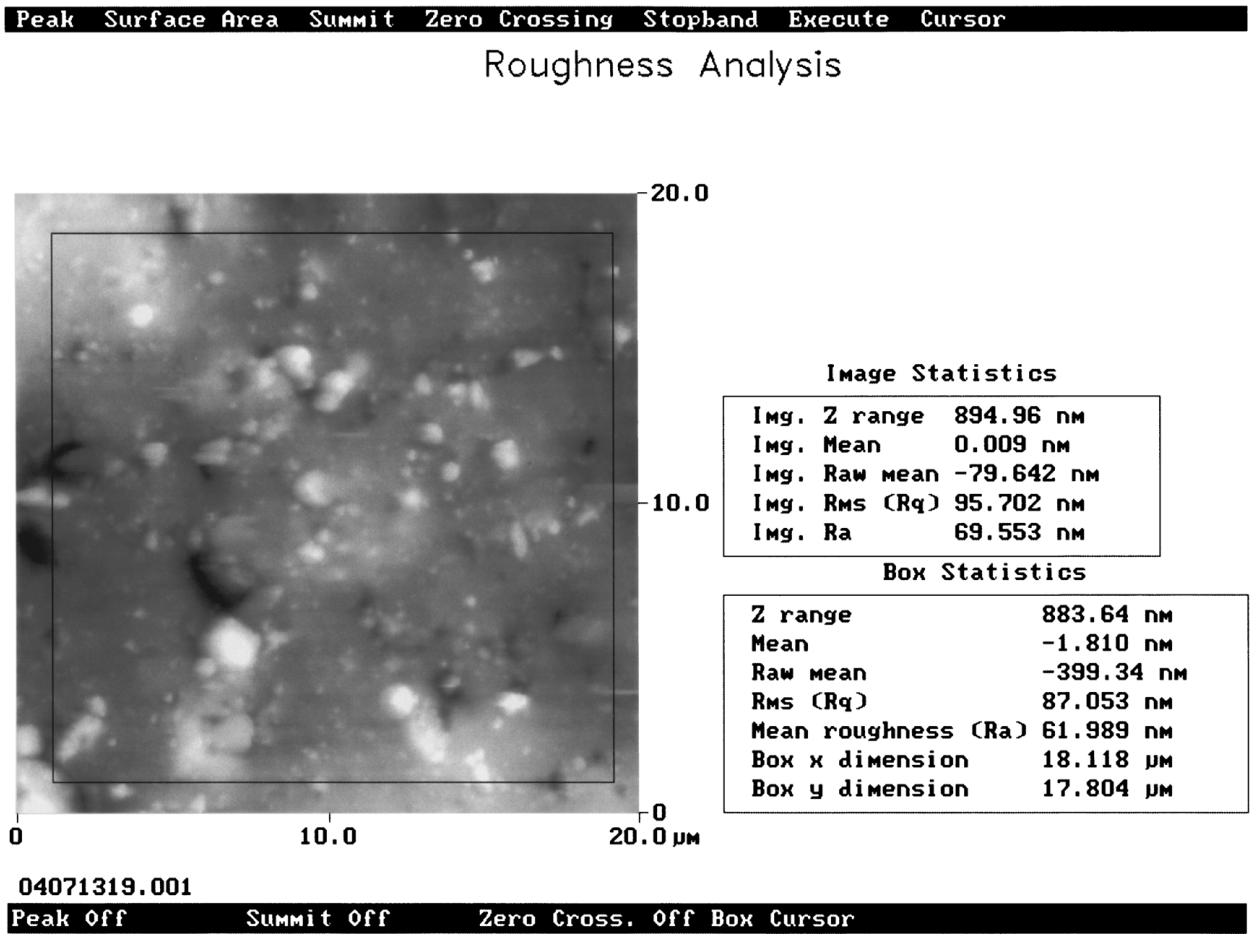

Figure 16 Roughness of the surface before aging.

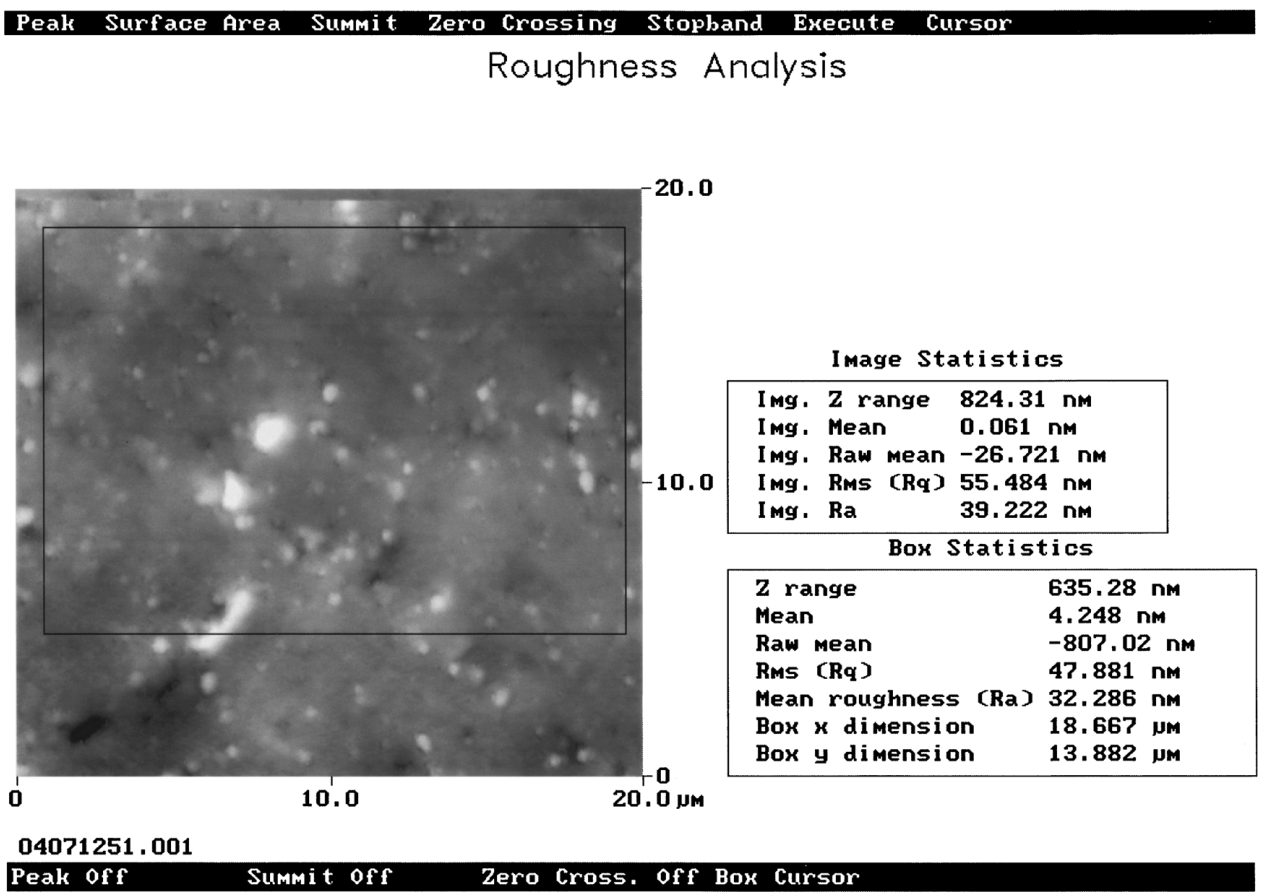

Figure 17 Roughness of the surface after aging.

4. Conclusions

Atomic Force Microscopy was used for a systematic study of the interaction between the fiber and the matrix in short melamine fiber reinforced EPDM rubber. It was observed that using AFM the role of bonding agent in improving the fiber-matrix interaction and the reasons for the improved strength and modulus of the composite after aging could be quantitatively analyzed. Section analysis of the images could be used as a tool for the quantitative evaluation of fiber geometry and fiber diameter in the composite. From the section analysis, fiber diameter was found to be 16 μm. Mechanical properties of the composites indicated that when the dry bonding system was added to the composite, tensile strength and modulus increased about 3 times as compared to that without bonding agent. Also, as resorcinol/hexamine ratio was increased from 5 : 3 to 10 : 6, there was an increment in tensile strength, though modulus and hardness remained almost the same. From the two-dimensional and three-dimensional topographic images of the composites with and without bonding agent, it was observed that addition of bonding agent created an interface, having thickness around 0.6 μm, between the fiber and the matrix. As the bonding agent ratio was increased from 5 : 3 : 15 to 10 : 6 : 15 (parts by weight), the width of the interface was increased from 1.79 μm to 5.39 μm, showing better fiber-matrix adhesion. Ageing of the composites at 150°C for 48 hours displayed an increase in the tensile strength, modulus and hardness of the composites. SEM and AFM studies showed that morphology of the composite was changed after ageing where the fiber was fully covered with the matrix. This improved adhesion between the fiber and the matrix was believed to be the reason for the increase in tensile strength and modulus of the composites after ageing.

Acknowledgement

The authors thank M/s BASF South East Asia Pte Ltd., Singapore for the free supply of melamine fiber. Thanks are also due to Indian Space Research Organisation for the financial assistance.

References

1. S. K DE and J. R. WHITE (eds.), "Short Fiber-Polymer Composites" (Woodhead Publishing Limited, Cambridge, England, 1996).
2. L. IBARRA and C. CHAMORRO, *J. Appl. Polym. Sci.* **37** (1989) 1197.
3. L. I. RUEDA, C. C. ANTON and M. C. TABERNERO RODRIGUEZ, *Polym.Comp.* **9** (1988) 198.
4. G. C. DERRINGER, *J. Elastoplast* **3** (1971) 230.
5. V. M. MURTY and S. K DE, *Rubber Chem. and Tech.* **55** (1982) 287.
6. D. K SETUA and S. K DE, *J. Mat. Sci.* **19** (1984) 983.
7. G. BINNIG, C. F. QUATE and CH. GERBER, *Phys. Rev. Lett.* **56** (1986) 930.
8. J. FOURNIER, H. MENARD, L. BROSSARD and Y. JUGNET, *J. Mater. Sci.* **31** (1996) 513.
9. C. M. DEMANET, S. LUYCKX, S. SHRIVASTAVA and I. WITCOMB, *J. Mater. Sci. Lett.* **15** (1996) 425.
10. A. K. FRITZSCHE, A. R. AREVALO, M. D. MOORE, C. J. WEBER, V. B. ELINGS, K. KJOLLER and C. M. WU, *J. Appl. Polym. Sci.* **46** (1992) 167.
11. J. FOURNIER, H. MENARD, L. BROSSARD and Y. JUGNET, *J. Mater. Sci.* **31** (1996) 513.
12. R. HOWLAND and L. BENATAR, "A Practical Guide to Scanning Probe Microscopy" (Park Scientific Industries, 1997).
13. V. V. TSUKRUK, *Rubber Chem. Tech.* **70** (1997) 430.
14. S. GHOSH, D. KHASTGIR, A. K. BHOWMICK, S. BANDYOPADHYAY, G. J. P. KAO and L. KOK, *J. Mater. Sci. Lett.* **19** (2000) 2161.
15. J. HAUTOJARVI and A. LEIJALA, *J. Appl. Polym. Sci.* **74** (1999) 1242.
16. S. REBOUILLAT, J. C. M. PENG and J. B. DONNET, *Polymer* **40** (1999) 7341.
17. D. GORITZ, H. RAAB, J. FROHLICH and P. G. MAIER, *Rubber Chem. Tech.* **72** (1999) 929.
18. S. MASS and W. GRONSKI, *Kautsch. Gum. Kunst.* **47** (1994) 409.
19. W. NIEDERMEIER, H. RAAB, J. STIERSTORFER, S. KREITMEIER and D GORITZ, *ibid.* **47** (1994) 799.
20. H. RAAB, J. FROHLICH and D. GORITZ, *ibid.* **53** (2000) 13.
21. W. NIEDERMEIER, H. RAAB, P. MAIER, S. KREITMEIER and D. GORITZ, *ibid.* **48** (1995) 611.
22. J. B. DONNET, E. CUSTODERO and TONG KUAN WANG, *ibid.* **49** (1996) 274.
23. D. TRIFONOVA-VAN HAERINGEN, H. SCHONHERR, G. J. VANCSO, L. VAN DER DOES, J. W. M. NOORDERMEER and P. J. P. JANSSEN, *Rubber Chem. Tech.* **72** (1999) 862.
24. M. GANTER, R. BRANDSCH, Y. THOMANN, T. MALNER and G. BAR, *Kautsch. Gum. Kunst.* **52** (1999) 717.
25. S. MAAS, R. LAY and W. GRONSKI, *ibid.* **49** (1996) 166.
26. R. S. RAJEEV, A. K. BHOWMICK and S. K. DE, *Polymer Composites* (communicated).
27. Technical Literature. BASOFIL Fiber (BASF Corporation, USA, 1999).

Received 10 August
and accepted 14 August 2000